

Onset of flux-bundle migration into superconducting niobium strips

Vincent Jeudy* and Denis Limagne

*Groupe de Physique des Solides (UMR 7588 CNRS) Tour 23, Universit es Paris 7 et Paris 6, 4 Place Jussieu,
75251 Paris Cedex 05, France*

(Received 3 May 1999)

Penetration of magnetic flux into type-II superconducting Nb strips is observed by a flux jump readout technique. To investigate the effect of the geometry, strips of different width are subjected to an increasing perpendicular magnetic field. We demonstrate that conventional geometrical barrier models cannot account for the onset of the flux migration into the strip volume. The migration starts for a local magnetic field at the strip equator higher than H_{c1} , allowing the irreversible penetration of the mixed state on the edges. The flux entry consists of flux bundles, each of them containing several hundreds of flux quanta. [S0163-1829(99)02134-7]

I. INTRODUCTION

Magnetic properties of type-II superconductors have recently received a renewed interest, in particular, the effect of the sample geometry on the properties of the mixed state is being actively investigated. Direct observations of the magnetic-flux distribution¹⁻³ on the top of flat samples placed in an increasing perpendicular magnetic field reveal that the flux does not necessarily enter gradually from the sample edges, as suggested by critical state models.⁴ Indeed, some magnetic flux can be unfastened from the edges and found in the sample center.

The role of geometry on the magnetization of high demagnetizing factor samples was first stressed by Clem, Huebener, and Gallus⁵ and Fortini and Paumier⁶ for type-I superconductors and more recently by Zeldov *et al.*⁷ for type-II superconductors. These authors calculated the energy associated with the presence of a normal-state domain in a diamagnetic volume. They have shown that over a large range of applied magnetic field, the normal domain energy is at its minimum at the strip center, albeit an edge energy barrier prevents the spontaneous flux migration from the edges.

Nevertheless, for an infinitely long superconducting strip of width L_x and thickness L_y , in presence of an applied magnetic field parallel to L_y , the models of Refs. 5, 6, and 7 propose different configurations of the flux lines penetrating on the strip edges, prior to the onset of the flux migration. This modifies the different energy contributions associated with the normal domain and leads to rather disconnected predictions concerning the onset of the flux migration into the volume. For a rectangular diamagnetic cross section, the applied magnetic field value H_m corresponding to the onset of the irreversible flux migration is given⁷ by $H_m \approx H_{c1} \sqrt{2L_y/L_x}$ while for an elliptical diamagnetic cross section, the migration starts⁵ for $H_m \approx H_{c1} L_y/L_x$.

To our knowledge, no systematic measurements exist of the migration onset for type-II superconductors. In this paper, we study the flux penetration into three rectangular-shaped superconducting Nb strips, cut out of the same foil and having different widths (L_x). The flux penetration is detected by a flux jump readout technique. The applied magnetic field corresponding to the flux jump detection onset is measured and compared to theoretical predictions. We show

that the irreversible installation of a mixed-state flux structure on the strip edges, disregarded in the geometrical metastability models, has to be considered to account for the onset of the flux migration towards the strip center. The magnetic field that must be applied to allow the circulation of a nondissipative pinning current on the strip edges is calculated in the elliptical diamagnetic cross-section case. A fit to the experimental data leads to the determination of the critical pinning current common to the three Nb strips. Finally, we show that the flux migration consists of flux bundles containing several hundreds of flux quanta.

II. EXPERIMENTAL

Our superconducting Nb samples are strips with rectangular cross section. Three different sizes ($900 \times 55 \times 23\,000$, $710 \times 55 \times 16\,000$, and $390 \times 55 \times 29\,000 \mu\text{m}^3$) were cut out from the same Goodfellow 99.9% pure and annealed 55- μm -thick foil. The Nb strips are plunged into a ^4He bath maintained at 4.2 K and subjected to a continuously increasing perpendicular magnetic field at a rate of 33 G/s. The flux penetration is detected by a fast-pulse acquisition system.⁸ The strips are placed against a branch of U-shaped pickup coil, connected via two transformers to a LeCroy HQV810 based pulse amplifier. A low frequency (10 kHz) cutoff of the bandwidth prevents the recording of the flux variations occurring at the applied magnetic-field sweeping rate: The reversible flux penetrations into the superconducting strips are therefore not detected. In contrast, the irreversible flux penetrations, whose high velocity is only limited by Eddy-current damping, are detected in real time by the measurement chain with $\approx 1\text{-}\mu\text{s}$ accuracy. Some hundreds of flux quanta⁹ have to jump simultaneously to produce pulses of amplitude higher than the electronic noise level. The detected signal is shaped and compared to a LeCroy MVL407-based discrimination threshold. Each pulse with amplitude higher than the discrimination threshold produces a transistor-transistor logic signal recorded by a computer. Two successive pulses contribute to two individual counts if their occurrence is separated by more than $\approx 10 \mu\text{s}$. The full acquisition system synchronizes the magnetic-field step rise

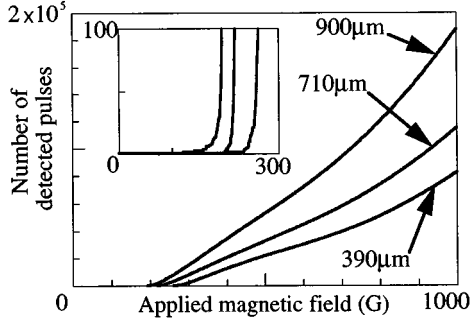


FIG. 1. Transition curves: cumulated number of detected pulses versus applied magnetic field for three samples of different sizes (see text). These curves were obtained for zero-field-cooled samples. $T=4.2$ K; Discrimination threshold 21 mV; sweeping rate: 33 G/s. Inset: Magnification featuring the flux jump detection onset.

with the opening of a gate during which flux pulses are detected and counted. Owing to the large inductance of the coil creating the magnetic field, the step command is integrated in a continuously varying field whose value rises linearly with the time.

III. ONSET OF THE IRREVERSIBLE FLUX MIGRATION

The integrated number of detected pulses as a function of the applied magnetic field (H_a) is shown in Fig. 1 for a discrimination threshold of 21 mV, set just above the electronic noise level. The flux jump detection starts for an applied magnetic field well above zero for the three sample sizes. Nevertheless, even if no flux jumps are recorded at low H_a , some flux penetration must occur since the beginning of the sweeping up, due to the quasi-infinite value of the local magnetic field on the strip edges. The vortices cut through the sharp rims of the strips without complete penetration into the edges and round off the flux-line curvature. As H_a increases, the mixed-state penetrates irreversibly deeper into the edges. The inset of Fig. 1 details the onset of the flux jump detection regime. A small number of flux jumps (10–30) are first detected and are followed by a massive flux penetration characterized by a high slope. The applied magnetic field H_m corresponding to the massive flux penetration onset is obtained by a linear extrapolation of the high slope to zero counts and then compared to the different geometrical barrier model predictions in Fig. 2. The lower critical field H_{c1} (4.2 K) = 1410 G has been taken from Ref. 10. The ratio H_m/H_{c1} decreases systematically as the sample width increases but the experimental points are well below all the theoretical predictions.

A. Geometrical barrier models

Let us discuss the different peculiarities of the geometrical barrier models. In the Zeldov *et al.* model,⁷ one computes the potential variation associated with the penetration of a single vortex into thin superconducting type-II strips. The diamagnetic volume is assumed to have a rectangular cross section so that the flux lines penetrating on the strip edges are straight lines. For a sample of width L_x and thickness L_y ($\lambda \ll L_y \ll L_x$ where λ is the magnetic-field penetration depth)

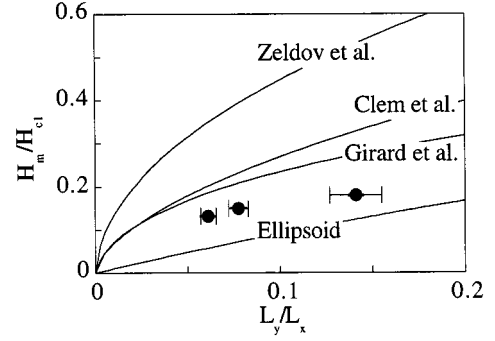


FIG. 2. Onset of the massive flux penetration. The migration magnetic field obtained experimentally (●) is compared with the predictions of different geometrical metastability models (see text) and with the case of an ellipsoid inscribed into the rectangular strip cross section.

subjected to a perpendicular applied magnetic field H_a , the shielding current averaged over the thickness is given by¹¹

$$J_y(X) = \frac{-cH_a}{2\pi L_y} \frac{X}{\sqrt{1-X^2}} \text{ for } |X| < 1 - \frac{L_y}{L_x},$$

$$\text{where } X = \frac{x}{L_x/2}. \quad (1)$$

The Meissner current exerts a position-dependant Lorentz force [$J_y(X)\phi_0/c$] on the vortex. The flux penetration starts when the resulting interaction energy compensates the line energy ($\varepsilon_0 L_y$) of a vortex. In absence of bulk pinning, the applied magnetic field has to be increased sufficiently high for the Lorentz force to reach $2\varepsilon_0/L_y$ near the strip edges ($1-|X|=L_y/L_x$). This is achieved for a local magnetic field value on the edges equal to H_{c1} and for an applied magnetic field given by

$$H_m \approx H_{c1} \sqrt{\frac{2L_y}{L_x}}. \quad (2)$$

Figure 2 shows that this predicted H_m/H_{c1} ratio is much higher than the present experimental results. The discrepancy is reinforced if one takes into account the effect of the bulk pinning. A formula similar to Eq. (2) was proposed in Ref. 12 for type-I superconductors. H_m was computed for a rectangular diamagnetic volume assuming that the migration starts for a local magnetic field at the strip equator equal to the thermodynamical critical field H_c . The comparison with the experimental data shows that if one neglects the rounding of the flux lines on the edges, the “edge effect” on the top and bottom edges leads to an infinite local magnetic field and to an overestimation of the penetration field.

The rounding of the flux lines on the edges is taken into account in the Clem, Huebener, and Gallus model.⁵ The diamagnetic volume is assumed to correspond to an ellipsoid inscribed in the strip’s rectangular cross section. The Gibbs free energy against the irreversible penetration of a normal domain is computed, in the two-dimensional (2D) case by conformal mapping, taking into account three energy contributions: (i) the line energy of the normal domain (ΔG_{in}) which increases with the thickness of the diamagnetic ellip-

soid when the vortex is moved from an edge towards the strip center, (ii) the magnetic energy generated by the domain outside the superconductor (ΔG_{out}) which tends to push the domain outside the sample volume, and (iii) The work (W_a) done by the source generating the applied magnetic field when the domain is introduced into the strip volume. The corresponding force tends to move the normal domain towards the strip center. The total Gibbs free energy depends on the geometrical dimensions of the strip, on the value of the applied magnetic field and on the size of the penetrating normal domain. This model, first developed to describe the flux penetration onset into type-I superconductors, is extended to the case of the migration of a single vortex in type-II superconducting strips. The applied magnetic field corresponding to the migration onset is given by

$$H_m = H_{c1} \frac{L_y}{L_x + L_y} \left(1 + \frac{2}{\ln \kappa} \frac{\sqrt{L_x \lambda}}{L_y} \right), \quad (3)$$

where λ and κ are respectively the London penetration length and the Ginzburg-Landau parameter. This formula is valid for $2\sqrt{L_x \lambda}/L_y \ll 1$, i.e., for high values of L_y/L_x . In the plot λ is taken equal to 480 Å (Ref. 13) and κ equal to 1.1. Since κ is neighboring 1.0 for niobium, the position of the curve is very sensitive to small κ fluctuations. An adjustment of the curve through the experimental H_m/H_{c1} ratio leads to $\kappa \approx 1.25$ which is higher than the value measured in Refs. 10 and 13. A lower κ sets the prediction at a position higher than the experimental measurements. This may be due to the overestimation, in the 2D case, of the magnetic-field energy outside the superconductor (ΔG_{out}). It is interesting to note that if ΔG_{out} is neglected, the flux penetration starts for a local magnetic-field value at the equator H_{eq} equal to H_{c1} (Ref. 14).

A more general approach was proposed by Fortini and Paumier⁶ for type-I superconductors, in which the remaining diamagnetic volume before flux migration was not chosen arbitrarily. They calculate the free energy associated with the presence of a normal domain in a general-shaped diamagnetic volume and neglect the magnetic energy contribution outside the superconductor. They show that the penetration of a normal domain is allowed when there is a full path joining the sample border and the center where the local magnetic field can be equal to H_c . As an applied magnetic field is increased, this condition is first satisfied in the sample center and then on the sample border. For a rectangular-shaped sample, the flux migration only starts when the intermediate state growing from the top and from the bottom of the strip edges meets at the strip equator allowing the local magnetic field to reach H_c . The migration magnetic field H_m depends on edge flux structure that remains to be determined. In Ref. 15, the shape of the wall separating the diamagnetic volume from the edge flux bearing zones and the migration field are calculated by conformal mapping, the intermediate state edge structure being assimilated to a normal metal. For a comparison with the Nb experimental data, H_c is substituted by H_{c1} . As in the two previously described geometrical metastability models, the predicted migration fields (see Fig. 2) remain higher than experimental results.¹⁶

B. Irreversible installation of the mixed state on the strip edges

At the onset of flux migration, the demagnetizing factor of the remaining diamagnetic volume must be higher than predicted by Ref. 15, i.e., the curvature of the flux lines near the strip equator must be higher than predicted by making a reversible flux penetration assumption. Indeed, for type-II superconductors, it is well known that the installation of the mixed state is not reversible. In the flux creep regime, the flux lines are able to move when the driving force becomes equal to the pinning force $F_p = \phi_0 J_c / c$, where ϕ_0 is the flux quantum and J_c is the nondissipative current flowing through the mixed state and shielding the external magnetic field. In the perpendicular geometry, the driving force exerted on the flux lines penetrating on the strip edges is not constant over the flux-line length. As the applied magnetic field is increased, the driving force exerted on a flux line near the top and the bottom of the strip is higher than the driving force exerted near the equator resulting in a deeper flux penetration towards the strip center near the top and the bottom of the strip. The unpinning condition is easier to reach near the top/bottom than near the strip equator, reinforcing the curvature of the flux lines near the strip equator. In the following, we will assume that at the migration onset, the remaining diamagnetic volume corresponds to an ellipsoid inscribed in the rectangular strip cross section.

The irreversible flux penetrations on the edges also modify the local magnetic field value that has to be reached on the strip equator for the flux to start to migrate toward the center. At the onset of the migration, the local magnetic field at the strip equator (H_{eq}) must reach (H_{c1}) plus a magnetic-field value (H_{cp}) sufficiently high to install the mixed state on the strip edges, i.e., to establish the circulation of a pinning current J_c between the rectangular and the elliptical cross section:

$$H_{\text{eq}} = H_{c1} + H_{cp}. \quad (4)$$

Let us calculate the magnetic field which has to be reached on the strip equator so that the mixed state fills the full strip volume outside the inscribed elliptical diamagnetic volume. This magnetic field can be calculated from the Biot and Savart law. For symmetry reasons, it is directed along the thickness of the strip. The contribution of each current element ($J_c ds$) to the magnetic field component directed along the thickness is given by

$$H_y = \frac{J_c ds}{2\pi r} \sin \theta, \quad (5)$$

where r is the distance between the current element location and the strip equator, and $\sin \theta$ is the magnetic-field projection along the thickness. The current density J_c , assumed to be constant, is circulated in the opposite direction on both sides of the strip (see Fig. 3). Consequently, the magnetic fields generated by those two currents have opposite contributions. Integration of Eq. (5) over the volume filled by the mixed state leads to total magnetic field equal to

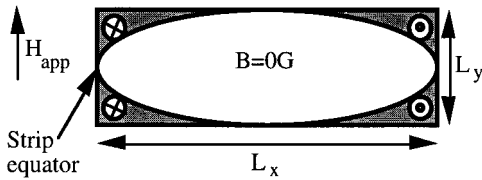


FIG. 3. Current distribution in the strip before the onset of the irreversible flux migration. The pinning current J_c is flowing on the edges of the strip, between the rectangular strip cross section and the inscribed diamagnetic ellipsoid.

$$H_{cp} = \frac{L_y J_c}{2\pi} \left[\ln\left(\frac{L_x}{L_y}\right) - 1 - \ln 2 \right] \quad (6)$$

for $L_x \gg L_y$. Figure 4 shows a comparison between the experimental data and Eq. (6). Since the three samples have been cut from the same thin foil, the value of their critical current density should be the same. The best fit of the experimental data leads to $J_c \approx 1.6 \times 10^6$ A/cm² which is the only free parameter.

An alternative measurement of the pinning current density was obtained from a zero-field-cooled dc magnetization measurement. A strip ($1000 \times 55 \times 15\,000 \mu\text{m}^3$), cut out of the same Nb Goodfellow foil, was cooled down to 4.1 K. To remove geometrical effects, the external magnetic field was applied parallel to the strip surface. The magnetization measurements were performed with a Quantum Design superconducting quantum interference device (SQUID) magnetometer and are shown in Fig. 5. As the external magnetic field increases from zero, the initial slope is constant, indicating that the sample remains fully diamagnetic. For the calibration of the SQUID magnetometer, the initial slope was set to -1 . The curve begins to deviate from the linear dependence when the external magnetic field reaches the lower critical field H_{c1} . The experimental value ($H_{c1} = 1250 \pm 250$ G) presents a large error but is similar to the value ($H_{c1} = 1413$ G) given in Ref. 10. The pinning current was determined following the critical state model of C. P. Bean.⁴ For an applied magnetic field higher than H_{c1} , the magnetic flux enters inside the sample volume through its border. The critical pinning current, assumed to be constant, flows in a su-

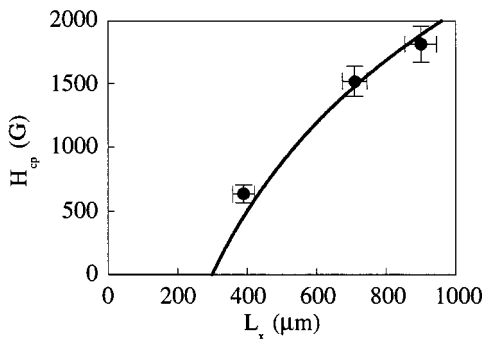


FIG. 4. Local magnetic field at the strip equator (H_{cp}) generated by the circulation of the pinning current J_c . The experimental values of H_{cp} are calculated using the values of the applied magnetic field corresponding to migration onset (H_m), the demagnetizing factor of an inscribed ellipsoid and Eq. (4). The continuous line is the best fit of Eq. (6) to the experimental points and leads to $J_c = 1.6 \times 10^6$ A/cm².

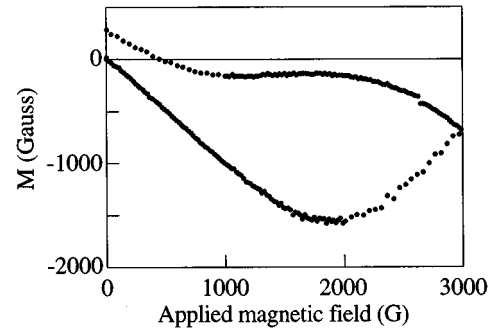


FIG. 5. Magnetization curve obtained with a dc SQUID. The niobium strip ($1000 \times 55 \times 15\,000 \mu\text{m}^3$) is subjected to a parallel magnetic field, $T = 4.1$ K. The pinning current J_c is determined via the critical state model of Bean (Ref. 4).

perfacial layer to ensure the screening of the external field from the sample center. The flux density within the sample decreases linearly from the applied magnetic-field value at surface to zero at the boundary of the Meissner state central region. When the applied magnetic field increases, the magnetization decreases until the flux reaches the center of the sample. This appears for an applied magnetic field $H^* = J_c L_y$ and a magnetization value equal to $M_{\min} = -1/2 H^*$. Figure 5 indicates that $M_{\min} = -1540$ G is obtained for $H^* = 1870$ G. Those two independent measurements lead to critical pinning current density values respectively equal to 0.54×10^6 A/cm² and 0.89×10^6 A/cm².

Despite the crude assumption made about the pinning current density, and the arbitrary choice of the demagnetizing factor, these two J_c values are proximate to the one obtained by fitting Eq. (6). This indicates that, for our samples aspect ratio, the remaining diamagnetic volume at the onset of the flux migration can be approximated to an ellipsoid inscribed into the strip rectangular cross section. That is to say, in comparison with the reversible case of Ref. 15, the irreversible installation of the mixed state on the edges increases the curvature of the flux lines and advances the onset of the flux migration. The few flux jumps detected before the migration field (see Fig. 1) probably reflect collective jumps of vortices on the strip edges.

At the onset of the flux migration, the local magnetic field at the strip equator is higher than H_{c1} . As shown in Eq. (6), the effect of the installation of the critical state on the edges is reduced when L_x/L_y decreases. For a large L_x/L_y ratio, the magnetic field generated on one side of the strip is essentially determined by the contribution of the currents circulating on the same side [see Eq. (5)]. In contrast to this, when the sample aspect ratio is sufficiently reduced, the effect of the currents circulating on the opposite side tends to be more important and to reduce the value of the magnetic field. The negative value of H_{cp} obtained in Eq. (5) for $L_x/L_y < 4.2$ shows the limitations of the elliptical diamagnetic volume assumption. A rigorous determination of the migration field should include the calculation of the flux profile and thermodynamical potential evolution during the applied magnetic field increase, taking into account the pinning of vortices. The edge pinning effect on the onset of the flux migration should be more pronounced for high-temperature superconductors than for niobium because of their rather low H_{c1} value and quite high pinning currents.

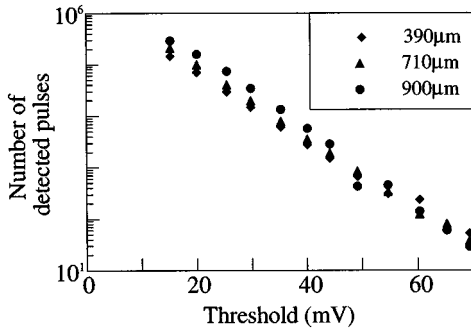


FIG. 6. Number of detected pulses versus threshold for the three different strip widths. The applied magnetic field has been swept up to 1000 G. These curves have been obtained with flux trapped into the samples.

IV. SIZE OF THE MIGRATING FLUX BUNDLES

For type-II superconductors it is usually assumed, as in Refs. 5 and 7, that the flux migration from the strip edges towards the center is achieved by single flux quanta. However, flux droplet penetration was observed in NbSe₂ (Ref. 3) by the Bitter decoration technique as well as in Nb films with an array of microscopical Hall probes.¹⁷

As described previously, the flux jump detection technique is not sensitive to the penetration of single vortices: several hundreds of quanta have to jump simultaneously to produce pulses whose amplitudes are higher than the electronic noise level. The fact that signals are detected, almost over all the sweeping-up range, demonstrates that the flux migration is achieved by the simultaneous jump of a large number of flux quanta. The average size of a flux bundle can be crudely estimated from the total number of counts recorded during the sweeping up of the magnetic field. As shown on Fig. 6, the number of detected pulses increases when the detection threshold is reduced. The exponential extrapolation to zero threshold gives an estimation of the total number of flux bundles F which have penetrated the strip during the magnetic field variation. F was determined by taking the data obtained at 21 mV with samples free of trapped flux (Fig. 1) and the exponential slopes obtained from Fig. 6 for samples containing trapped flux. The number of flux quanta N present in the sample volume is assumed to be a linear function of the applied magnetic field (H_a), i.e., $N(H_a) \sim H_a - H_m$, where H_m is the migration field. The number of flux quanta having already migrated at H_a is given by

$$N(H_a) = N(H_{c2}) \frac{H_a - H_m}{H_{c2} - H_m}, \quad (7)$$

TABLE I. Rough estimation of number of flux quanta per flux bundle (ϕ/ϕ_0) for the three strip widths.

L_x (μm)	ϕ/ϕ_0
390	240
710	140
900	120

where the number of flux quanta migrated when H_a reaches H_{c2} , $N(H_{c2}) = H_{c2}L_xL_z/\phi_0$, is obtained by flux conservation. The H_{c2} value (= 2590 G) was taken from Ref. 10. The number of quanta per flux bundle is then given by

$$\frac{\phi}{\phi_0} = \frac{N(1000 \text{ G})}{F(L_x)}. \quad (8)$$

During the applied magnetic field increase, flux bundles are unfastened from the mixed-state structure present on the strip edges and move towards the strip center. The systematic dependency of the bundle size (shown in Table I) on the sample width indicates that the shape of the volume filled with the mixed state plays a crucial role in the unfastening process of the flux bundles. Moreover, recent measurements to be published in a forthcoming paper show that the size of the flux bundles varies with the sweeping rate of the applied magnetic field, underlining the role of the flux creep rate on the edges.

V. CONCLUSION

The onset of flux migration into superconducting type-II Nb strips, subjected to a perpendicular magnetic field, is controlled by the installation of a critical state on the edges of the strip, and appears for a local magnetic field at the strip equator higher than H_{c1} . This is in contrast to the reversible flux installation hypothesis proposed in different geometrical barrier models. The local magnetic field at the strip equator, produced by the pinning currents flowing on the edges of the strip in the case of an elliptical diamagnetic volume was calculated. A comparison with the experimental determination of the onset of the flux migration allows the determination of the critical current common to three superconducting strips cut out from the same foil. The flux migration towards the strip center is in the form of flux bundles containing several hundreds of quanta, whose size depends on the structure of the critical state present on the strip edges.

ACKNOWLEDGMENTS

We are grateful to L. Legrand and M. Saint Jean for helpful discussions and to I. Rosenman for the SQUID measurements.

*Author to whom correspondence should be addressed. Electronic address: jeudy@gps.jussieu.fr

¹M. V. Indenbom, H. Kronmüller, T. W. Li, P. H. Kes, and A. A. Menovsky, *Physica C* **222**, 203 (1994).

²S. T. Stoddart, S. J. Bending, A. K. Geim, and M. Henini, *Phys. Rev. Lett.* **71**, 3854 (1993).

³M. Marchevsky, L. A. Gurevich, P. H. Kes, and J. Aarts, *Phys. Rev. Lett.* **75**, 2400 (1995).

⁴C. P. Bean, *Phys. Rev. Lett.* **8**, 250 (1962).

⁵J. R. Clem, P. Huebener, and D. E. Gallus, *J. Low Temp. Phys.* **12**, 449 (1973).

⁶A. Fortini and E. Paumier, *Phys. Rev. B* **14**, 55 (1976).

⁷E. Zeldov, A. I. Larkin, V. B. Geshkenbein, M. Konczykowski, D. Mayer, B. Khaykovich, V. M. Vinokur, and H. Shtrikman, *Phys. Rev. Lett.* **73**, 1428 (1994).

⁸A. Hrisoho and G. Waysand, *Nucl. Instrum. Methods Phys. Res.*

- 214**, 415 (1983).
- ⁹V. Jeudy, D. Limagne, and G. Waysand, *Europhys. Lett.* **16**, 491 (1991).
- ¹⁰T. F. Stromberg and C. A. Swenson, *Phys. Rev. Lett.* **9**, 370 (1962).
- ¹¹E. H. Brandt, *Phys. Rev. B* **46**, 8628 (1992).
- ¹²J. Provost, E. Paumier, and A. Fortini, *J. Phys. F* **4**, 439 (1974).
- ¹³B. W. Maxfield and W. L. McLean, *Phys. Rev.* **139**, 1515 (1969).
- ¹⁴M. Benkraouda and J. R. Clem, *Phys. Rev. B* **53**, 5716 (1996).
- ¹⁵J.-P. Girard, E. Paumier, and A. Hairie, in *Proceedings of the 14th International Conference on Low Temperature Physics*, Otaniemi, Finland, 1975, edited by M. Krusius and M. Vuorio (North-Holland, Amsterdam, and American Elsevier, New York, 1975), Vol. 2, p. 199.
- ¹⁶As described in the “fanlike model,” A. Fortini, A. Hairie, and J.-P. Girard, *J. Math. Phys.* **20**, 2139 (1979); J. P. Girard, E. Paumier, and A. Hairie, *Phys. Rev. B* **21**, 2734 (1980), the predicted migration field could be reduced by taking into account the fine structure of the mixed state present on the edges, which would reduce the amount of flux penetrated on the edges as assumed with the normal-metal approximation.
- ¹⁷S. T. Stoddart, S. J. Bending, R. E. Somekh, and M. Henini, *Supercond. Sci. Technol.* **8**, 459 (1995).